A Sodalite-Type Porous Metal-Organic Framework with Polyoxometalate Templates: Adsorption and Decomposition of Dimethyl Methylphosphonate

ARTICLE *in* JOURNAL OF THE AMERICAN CHEMICAL SOCIETY · MARCH 2011

Impact Factor: 12.11 · DOI: 10.1021/ja109659k · Source: PubMed

8 AUTHORS, INCLUDING:

Feng Wei
Beijing University of Posts and Telecommuni…
60 PUBLICATIONS **638** CITATIONS
SEE PROFILE

Ya-Guang Chen
Northeast Normal University
104 PUBLICATIONS **1,038** CITATIONS
SEE PROFILE

JACS
JOURNAL OF THE AMERICAN CHEMICAL SOCIETY

COMMUNICATION

pubs.acs.org/JACS

A Sodalite-Type Porous Metal−Organic Framework with Polyoxometalate Templates: Adsorption and Decomposition of Dimethyl Methylphosphonate

Feng-Ji Ma, Shu-Xia Liu,* Chun-Yan Sun, Da-Dong Liang, Guo-Jian Ren, Feng Wei, Ya-Guang Chen, and Zhong-Min Su*

Key Laboratory of Polyoxometalate Science of the Ministry of Education, College of Chemistry, Northeast Normal University, Changchun, Jilin 130024, China

Supporting Information

ABSTRACT: A sodalite-type porous metal−organic framework with polyoxometalate templates, $H_3[(Cu_4Cl)_3(BTC)_8]_2[PW_{12}O_{40}]\cdot(C_4H_{12}N)_6\cdot 3H_2O$ (**NENU-11**; BTC = 1,3,5-benzenetricarboxylate), was obtained by a hydrothermal reaction. As a reasonable candidate for eliminating nerve gas, **NENU-11** displays good adsorption behavior for dimethyl methylphosphonate (15.5 molecules per formula unit). In virtue of the catalytic activity of polyoxometalate guests, this nerve gas mimic could be facilely decomposed by a hydrolysis reaction.

The construction and characterization of porous materials with versatilities have been the focus of intense research interest. Metal−organic frameworks (MOFs) are a new class of crystalline porous materials consisting of metal ions and organic ligands[1] that have high porosities and specific functionalities: catalysis,[2] magnetism,[3] separation,[4] and gas adsorption.[5] They not only offer high surface areas but also provide tunable pore shapes/sizes. As a consequence, they are allowed greater chemical alteration on a periodic scale and can be used as hosts for encapsulating other guest molecules to construct new multifunctional materials.

Polyoxometalates (POMs) are polyoxoanions of the early transition elements and have numerous advantageous properties.[6] Because of their various structures and symmetries, POMs have been incorporated into MOFs as guests or templates to construct novel hybrid materials.[7,8] These hybrid materials based on porous MOFs and POMs (shortened as PMOFs/POMs), which present intriguing structures, excellent properties, and corresponding applications, have received increasing attention. With the introduction of POM guests, MOFs have been fine-tuned for more specialized applications such as heterogeneous catalysis[9a] and adsorption.[9b] Furthermore, using POMs as templates in the fabrication of MOFs may afford brand-new hybrid compounds with wider functionalities. POMs can provide diverse shapes, sizes, charges, and symmetries for assembly of various MOFs, while the tailorable acid/base, redox, and catalysis propertyies of POMs also can optimize MOFs for targeted applications. Herein we utilized the Keggin-type polyoxoanion $[PW_{12}O_{40}]^{3-}$ as a template to construct a novel PMOF/POM, $H_3[(Cu_4Cl)_3(BTC)_8]_2[(C_4H_{12}N)_6PW_{12}O_{40}]\cdot 3H_2O$ (**NENU-11**; BTC = 1,3,5-benzenetricarboxylate), that exhibits a sodalite topology network and permanent porosity. **NENU-11**, which has entatic metal centers (EMCs) and multifunctional POM guests, shows great potential in the elimination of nerve gas. As a reasonable candidate, it not only displays good adsorption behavior for dimethyl methylphosphonate (DMMP), which is used extensively as a nerve gas simulant, but also realizes the decomposition of DMMP through a facile hydrolysis reaction.

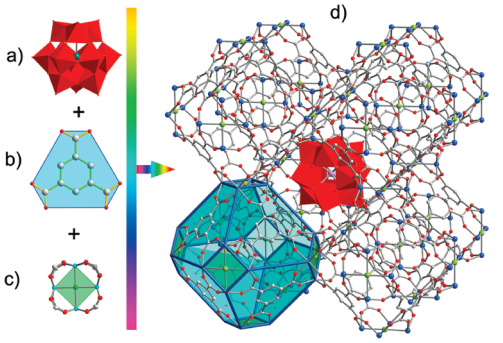

Figure 1. (a) Keggin polyanion. (b) Three-connected node and hexagonal face (blue) defined by a BTC ligand linked to six adjacent Cu^{2+} ions. (c) SBU and square face (green) defined by four Cu^{2+} ions. (d) Cube of eight sodalite-like truncated-octahedral cages sharing square faces. Hydrogen atoms and $(CH_3)_4N^+$ cations have been omitted for clarity. Cu (blue), O (red), C (gray), Cl (green), Keggin polyanion (red polyhedron).

NENU-11 can be readily synthesized in good yield (65%) by the hydrothermal reaction of $CuCl_2\cdot 2H_2O$, $Na_3PW_{12}O_{40}\cdot 12H_2O$, H_3BTC, and $(CH_3)_4NOH$ at 180 °C for 72 h. The cube-shaped crystals crystallized in the $Fm\bar{3}m$ space group. Single-crystal X-ray diffraction (XRD) analysis revealed that **NENU-11** exhibits a sodalite-type network in which the Keggin polyoxoanions $[PW_{12}O_{40}]^{3-}$ act as noncoordinating guests (Figure 1). Six $(CH_3)_4N^+$ cations are located around every $[PW_{12}O_{40}]^{3-}$ ion in the crystal structure, as confirmed by elemental analysis, atomic absorption spectra, and thermogravimetric analysis (TGA). Bond valence sum calculations indicated that the oxidation states of W, P, and Cu were 6+, 5+, and 2+, respectively. The extra anionic charge of the compound must be balanced by protons, which could not be directly located by single-crystal

Received: November 2, 2010
Published: March 03, 2011

dx.doi.org/10.1021/ja109659k | J. Am. Chem. Soc. 2011, 133, 4178–4181

XRD, as is often the case.[10] Thus, **NENU-11** was formulated as $H_3[(Cu_4Cl)_3(BTC)_8]_2[(C_4H_{12}N)_6PW_{12}O_{40}]\cdot 3H_2O$. Moreover, the phase purity of the as-synthesized sample was confirmed by elemental analysis and powder XRD (PXRD) (see the Supporting Information).

In **NENU-11**, the host framework adopts a square-planar $Cu_4(\mu_4\text{-Cl})$ secondary building unit (SBU) (Figure 1c) with a μ_4-Cl residing at the center of a square of four Cu atoms. All four Cu atoms in the SBU are five-coordinate with a perfect square-pyramidal geometry[11] ($\tau = 0$). The μ_4-Cl is located at the vertex of each square pyramid, with a Cu−μ_4-Cl distance of 2.538 (10) Å. The existence of Cl was confirmed by X-ray photoelectron spectroscopy (XPS) measurements in the Cl 2p region (198 eV) (see Figure S3 in the Supporting Information), and its content was quantitively determined by elemental analysis. The four Cu in the $Cu_4(\mu_4\text{-Cl})$ SBU are connected through the O atoms from eight surrounding BTC ligands (Figure S1a). In turn, each triangular BTC ligand is connected to three $Cu_4(\mu_4\text{-Cl})$ squares, generating a 3,8-connected network (Figure S2a). Intriguingly, each Cu in each SBU can act as an EMC, mimicking the coordinatively unsaturated iron active center of hemoglobin (Figure S4). Each Cu is ready to bind a substrate to achieve octahedral coordination.[10] The fundamental building unit of the framework is a truncated octahedron, outlined as Figure 1d. Every truncated octahedron presents a classic sodalite cage defined by six $Cu_4(\mu_4\text{-Cl})$ SBUs at the corners and eight BTC ligands on the faces (Figure S2b). The cube cage is about 10.8 Å × 10.8 Å × 10.8 Å (atom-to-atom distance), and the length of diagonal is 15.4 Å. The solvent-accessible volume of **NENU-11** calculated using PLATON[12] is 24.5%.

As a matter of fact, the sodalite topology has been observed in some reported MOFs, such as $[(Cu_4Cl)_3(TPB\text{-}3tz)_8]^{3-}$ [TPB-3tz =1,3,5-tri-*p*-(tetrazol-5-yl)phenylbenzene][13a] (Figure S5a), $[(Cu_4Cl)_3(TPT\text{-}3tz)_8]^{3-}$ [TPT-3tz =2,4,6-tri-*p*-(tetrazol-5-yl)-phenyl-*s*-triazine][13a] (Figure S5b), and $[(Cu_4Cl)_3(BTT)_8(H_2O)_{12}]^{3-}$ [BTT = 1,3,5-benzenetris(tetrazolate)][13b] (Figure S5c). Although the extended ligands in these compounds coordinate similarly to BTC, MOFs with sodalite topology constructed from $Cu_4(\mu_4\text{-Cl})$ and BTC have not been reported to date. We also tried best to obtain the independent framework without POMs but failed. When no $[PW_{12}O_{40}]^{3-}$ anions existed in this reaction system, only a small amount of $Cu_3(BTC)_2$ was obtained.[14] We further attempted to use other types of POMs (such as Dawson-type, Anderson-type, and Lindqvist-type) to construct this framework. However, the framework could not be maintained with other types of POMs under these conditions. The stability of **NENU-11** appears to be the result of the good match of the shape (approximately spherical), size (~10.4 Å), and symmetry (T_d) of the Keggin-type POMs with the MOF host. Thus, we believe that Keggin-type POMs actually may act as templates for the in situ formation of the framework.[15]

NENU-11 is insoluble in water and common organic solvents. It was stable under air atmosphere for more than 2 months, and no efflorescence was observed. The hydrothermal stability test showed that **NENU-11** retained intact after treatment with 100 °C water for 120 h. The TGA curve showed (Figure S6) a plateau before ~300 °C with a weight loss of <1% (calcd 0.64% for three water molecules). **NENU-11** was activated under vacuum (~10^{-6} mbar) at 200 °C for 12 h after refluxing in a saturated solution of NH_4Cl for 72 h. The elimination of $(CH_3)_4N^+$ in **NENU-11** was indicated by the disappearance of its characteristic peaks in the IR spectrum (Figure S7).

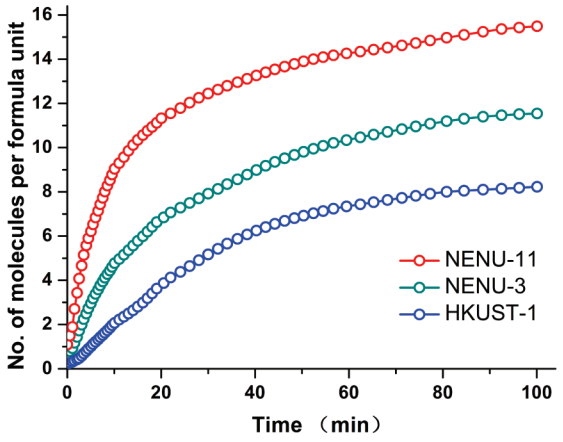

Figure 2. Variation of DMMP uptake over time for **NENU-11**, **NENU-3**, and HKUST-1 at 298 K and 1 bar under flowing He.

Furthermore, the elemental analysis further showed that no N was present in activated **NENU-11a**, the molecular formula of which can be denoted as $H_3[(Cu_4Cl)_3(BTC)_8]_2[H_6PW_{12}O_{40}]$. The activation process occurred without loss of structural integrity, as confirmed by PXRD studies (Figure S9). Activated **NENU-11a** was employed to study the porosity and adsorption properties.

The permanent porosity was evaluated by N_2 adsorption at 77 K. The N_2 adsorption isotherm displayed typical type-I adsorption behavior (Figure S11), confirming the presence of the microporous structure.[16] A N_2 uptake of 199 cm^3(STP) g^{-1} was observed, with a Brunauer−Emmett−Teller (BET) surface area of 572 $m^2\ g^{-1}$ and a Langmuir surface area of 806 $m^2\ g^{-1}$. The total pore volume was 0.39 $cm^3\ g^{-1}$. Applying Dubinin−Astakhov (DA) analysis[17] to the isotherm data showed that the pore size was distributed widely around 10.3 Å (Figure S12), which corresponds to the result from crystallographic structure analysis (10.8 Å).

DMMP has been used as a common simulant for type-G and type-X toxic nerve agents[18] because it has polarity and volatility similar to that of nerve gases such as sarin but is much safer to use. We assessed the potential validity of **NENU-11** for removal of nerve gas by DMMP adsorption. The dynamic capacity measurement was implemented at 298 K and 1 atm under flowing carrier gas (He) conditions. As indicated in Figure 2, **NENU-11** showed rapid adsorption of DMMP in the initial 20 min. The adsorbed amount of DMMP increased gradually over time, reaching 23.82 wt % (1.92 mmol g^{-1}) within 100 min. This value is equivalent to the adsorption of 15.5 DMMP molecules per formula unit (defined as the SBU). It is noteworthy that this value is superior to that of MOF-5 (6 DMMP molecules per formula unit),[19] for which BET surface area is 3362 $m^2\ g^{-1}$ and the pore volume is 1.18 $cm^3\ g^{-1}$.[20a] The considerable amount of adsorbed DMMP could be attributable to the remarkable structure of **NENU-11**. The presence of EMCs provides a strong interaction with DMMP through Cu−O bonds because of the appropriate complex stability constants of copper phosphate.[21] In principle, DMMP has three different functionalities (PCH_3, P═O, and $POCH_3$) that could be responsible for the H bonds. The extensive H bonding between DMMP and POMs together with DMMP and O of the framework may also increase the adsorption. After DMMP adsorption, the IR spectrum (Figure S8) of the resulting material (designated as **NENU-11a**) showed obvious characteristic

dx.doi.org/10.1021/ja109659k | *J. Am. Chem. Soc.* 2011, 133, 4178–4181

Table 1. N_2 and DMMP Adsorption Studies of NENU-11, NENU-3, HKUST-1, and MOF-5

	A_{BET}[a]	pore volume[b]	N_{DMMP}[c]	refs
NENU-11	572	0.39	15.5	this work
NENU-3	405	0.31	11.5	9b, this work
HKUST-1	1507	0.75	8.2	20b, this work
MOF-5	3362	1.18	6	19,20a

[a] BET surface area in $m^2\ g^{-1}$ obtained from N_2 isotherms at 77 K. [b] In $cm^3\ g^{-1}$. [c] Numbers of DMMP molecules adsorbed per formula unit (defined as the SBU, Cu_4 for **NENU-11**, Cu_2 for **NENU-3**, Cu_2 for HKUST-1, and Zn_4 for MOF-5), as obtained from the dynamic capacity measurements of DMMP at 298 K.

peaks (e.g., metal−phosphate or C−O[21,22]), confirming that DMMP molecules strongly interact with the sorbent.

To further investigate the relationship between the structure and DMMP adsorption, we also measured the DMMP adsorption of other materials under the same conditions for comparison with **NENU-11**. To date there is no other MOF formed directly from $Cu_4(\mu_4\text{-Cl})$ and BTC, so we first chose HKUST-1 $[Cu_3(BTC)_2]$, which is formed by Cu and BTC too. It was found that HKUST-1 adsorbs 8.2 DMMP molecules per formula unit at 298 K (Figure 2). In comparison with MOF-5, HKUST-1 reaches a higher DMMP adsorption despite its lower BET surface area ($1507\ m^2\ g^{-1}$) and pore volume ($0.75\ cm^3\ g^{-1}$).[20b] This occurs mainly because solvent molecules in HKUST-1 can be removed to give coordinatively unsaturated metal centers (UMCs),[14] which are similar to EMCs and could increase the absorption capability. In addition, we measured the dynamic DMMP adsorption of **NENU-3** $\{(C_4H_{12}N)_2[Cu_{12}(BTC)_8\cdot 12H_2O][HPW_{12}O_{40}]\cdot 25H_2O\}$,[9] which was constructed from HKUST-1 and a polyoxoanion $[PW_{12}O_{40}]^{3-}$. As shown in Figure 2, **NENU-3** adsorbs 11.5 DMMP molecules per formula unit at 298 K, with the lowest BET surface area ($405\ m^2\ g^{-1}$) and pore volume ($0.31\ cm^3\ g^{-1}$). This value is higher than that of either MOF-5 or the parent MOF HKUST-1 but lower than that of **NENU-11** (Table 1). Because of the higher molecular weights of POMs, the adsorption amount of DMMP on a mass basis for **NENU-11** is lower. MOF-5 with its larger pore volume adsorbs 0.90 g of DMMP/g of sorbent,[19] HKUST-1 0.83 g g^{-1}, and **NENU-11** 0.24 g g^{-1}, respectively. (Table S3) However, POM guests cannot be ignored for their contribution to the DMMP adsorption. The adsorption amount on a volume basis for **NENU-11** is competitive with that of the single MOFs. (Table S3) MOF-5 adsorbs 0.53 g of DMMP/cm^3 of adsorbent, HKUST-1 0.79 g cm^{-3}, and **NENU-11** 0.55 g cm^{-3}. Clearly, all of these results indicate that POMs play an important role in the adsorption of DMMP. Simultaneously, **NENU-11** can adsorb larger amounts of DMMP than **NENU-3**, perhaps because of its higher surface area and pore volume.

In order to investigate DMMP decontamination under conditions close to ambient, the effect of humidity was considered. We performed the DMMP adsorption measurements at relative humidities (RHs) of 5, 10, 20, 50, and 80%. In combination with water adsorption equilibria at various RHs (Figure S13), it was found that the presence of water vapor affected the adsorption of DMMP to some extent (Figure S14). In comparison with the adsorption at RH = 0, the total amount adsorbed decreased as the RH increased. Still, the main contribution to the total amount should come from DMMP, which could be attributed to the higher polarizability of DMMP (10.43) than water (1.45), resulting in stronger interactions with the sorbent.

Scheme 1. Hydrolysis of DMMP

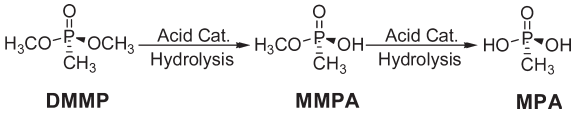

DMMP desorption measurements performed on **NENU-11a** by outgassing showed that the amount of DMMP decreased slowly over time (Figure S15). This can be satisfactorily explained by the strong interaction between DMMP molecules and the sorbent. Decomposition or decontamination is an important issue for nerve gas because of its toxicity. Taking into account the fact that Keggin-type POMs have been widely used as acid catalysts for hydrolysis of esters[9a,23] and furthermore that the decomposition of DMMP has been carried out by hydrolysis, including acid hydrolysis and basic hydrolysis,[24] we put **NENU-11a** with adsorbed DMMP into water and monitored the system using gas chromatography coupled with mass spectrometry (GC−MS). The detection of methyl alcohol demonstrated the hydrolysis of DMMP. The hydrolysis products were methyl alcohol, methyl methylphosphonic acid (MMPA), and methylphosphonic acid (MPA) (Scheme 1). The conversion of DMMP analyzed by GC−MS was 34% at room temperature. It was found that the conversion increased gradually with temperature, reaching 93% at 50 °C. Continued heating produced little change in the conversion. After 8 h, **NENU-11a** was filtered, washed with water, and then regenerated under vacuum at 200 °C for 12 h. After more than 10 cycles, the PXRD patterns showed that the positions of the main peaks at low angles remained consistent (Figure S10), indicating that the structural integrity was kept. In addition, according to the tiny amount of methyl alcohol in the exhaust gas, GC−MS analysis showed that a weak hydrolysis occurred during the adsorption process at higher RH (see the Supporting Information). Both the reactivity of DMMP on **NENU-11a** and the high stability of the latter highlight its possible use in decontamination, filtration, or removal of toxic nerve agents. In particular, the catalytic hydrolysis provides a more facile and environmentally friendly approach for the decomposition of nerve gas than the previous approaches, such as thermal reaction.

In conclusion, a novel PMOF/POM (**NENU-11**) with sodalite topology was obtained by the hydrothermal reaction of simple reagents. Porous **NENU-11** displayed its potential application in the removal of nerve gas by its performance in DMMP adsorption measurements. Furthermore, its excellent stability and powerful POM guests make it facile for the decomposition of nerve gas mimics. The hybridization of POMs and PMOFs presented here provides a promising approach for the design and construction of this kind of multifunctional material. By virtue of the porosity of MOF hosts and the numerous properties of POM guests, these materials may find more applications in other areas, such as gas-phase catalysis.

■ ASSOCIATED CONTENT

Supporting Information. Experimental details, X-ray crystallographic data (CIF), and additional characterization data. This material is available free of charge via the Internet at http://pubs.acs.org.

dx.doi.org/10.1021/ja109659k | J. Am. Chem. Soc. 2011, 133, 4178–4181

AUTHOR INFORMATION

Corresponding Author
liusx@nenu.edu.cn

ACKNOWLEDGMENT

This work was supported by the NSFC (Grants 20871027 and 20973035), the Program for New Century Excellent Talents in University (NCET-07-0169), Fundamental Research Funds for the Central Universities (Grant 09ZDQD0015), and the Program for Changjiang Scholars and Innovative Research Team in University.

REFERENCES

(1) (a) Long, J. R.; Yaghi, O. M. *Chem. Soc. Rev.* **2009**, *38*, 1213. (b) Férey, G. *Chem. Soc. Rev.* **2008**, *37*, 191. (c) Kitagawa, S.; Kitaura, R.; Noro, S. *Angew. Chem., Int. Ed.* **2004**, *43*, 2334.

(2) (a) Seo, J. S.; Whang, D.; Lee, H.; Jun, S. I.; Oh, J.; Jeon, Y. J.; Kim, K. *Nature* **2000**, *404*, 982. (b) Zou, R.; Sakurai, H.; Xu, Q. *Angew. Chem., Int. Ed.* **2006**, *45*, 2542.

(3) (a) Halder, G. J.; Kepert, C. J.; Moubaraki, B.; Murray, K. S.; Cashion, J. D. *Science* **2002**, *298*, 1762. (b) Cheng, X. N.; Zhang, W. X.; Lin, Y. Y.; Zheng, Y. Z.; Chen, X. M. *Adv. Mater.* **2007**, *19*, 1494.

(4) (a) Matsuda, R.; Kitaura, R.; Kitagawa, S.; Kubota, Y.; Belosludov, R. V.; Kobayashi, T. C.; Sakamoto, H.; Chiba, T.; Takata, M.; Kawazoe, Y.; Mita, Y. *Nature* **2005**, *436*, 238. (b) Chen, B.; Liang, C.; Yang, J.; Contreras, D. S.; Clancy, Y. L.; Lobkovsky, E. B.; Yaghi, O. M.; Dai, S. *Angew. Chem., Int. Ed.* **2006**, *45*, 1390.

(5) (a) Eddaoudi, M.; Kim, J.; Rosi, N.; Vodak, D.; Wachter, J.; O'Keeffe, M.; Yaghi, O. M. *Science* **2002**, *295*, 469. (b) Yoon, J. W.; Jhung, S. H.; Hwang, Y. K.; Humphrey, S. M.; Wood, P. T.; Chang, J. S. *Adv. Mater.* **2007**, *19*, 1830.

(6) (a) Pope, M. T.; Muller, A. *Angew. Chem., Int. Ed. Engl.* **1991**, *30*, 34. (b) Hill, C. L. *Chem. Rev.* **1998**, *98*, 1. (c) Long, D. L.; Burkholder, E.; Cronin, L. *Chem. Soc. Rev.* **2007**, *36*, 105.

(7) (a) Inman, C.; Knaust, J. M.; Keller, S. W. *Chem. Commun* **2002**, 156. (b) Férey, G.; Mellot-Draznieks, C.; Serre, C.; Millange, F.; Dutour, J.; Surble, S.; Margiolaki, I. *Science* **2005**, *309*, 2040. (c) Duan, C. Y.; Wei, M. L.; Guo, D.; He, C.; Meng, Q. J. *J. Am. Chem. Soc.* **2010**, *132*, 3321. (d) Zheng, S. T.; Zhang, J.; Yang, G. Y. *Angew. Chem., Int. Ed.* **2008**, *47*, 3909. (e) Yu, R. M.; Kuang, X. F.; Wu, X. Y.; Lu, C. Z.; Donahue, J. P. *Coord. Chem. Rev.* **2009**, *253*, 2872.

(8) (a) Zhao, X. Y.; Liang, D. D.; Liu, S. X.; Sun, C. Y.; Cao, R. G.; Gao, C. Y.; Ren, Y. H.; Su, Z. M. *Inorg. Chem.* **2008**, *47*, 7133. (b) Liu, S. X.; Xie, L. H.; Gao, B.; Sun, C. Y.; Su, Z. M. *Chem. Commun.* **2005**, 5023.

(9) (a) Sun, C. Y.; Liu, S. X.; Liang, D. D.; Shao, K. Z.; Ren, Y. H.; Su, Z. M. *J. Am. Chem. Soc.* **2009**, *131*, 1883. (b) Ma, F. J.; Liu, S. X.; Liang, D. D.; Ren, G. J.; Su, Z. M. *Eur. J. Inorg. Chem.* **2010**, 3756.

(10) Ma, S.; Zhou, H. C. *J. Am. Chem. Soc.* **2006**, *128*, 11734.

(11) Addison, A. W.; Rao, T. N.; Reedijk, J.; van Rijn, J.; Verschoor, G. C. *J. Chem. Soc., Dalton Trans.* **1984**, 1349.

(12) Spek, A. L. *PLATON 99: A Multipurpose Crystallographic Tool*; Utrecht University: Utrecht, The Netherlands, 1999.

(13) (a) Dincă, M.; Dailly, A.; Tsay, C.; Long, J. R. *Inorg. Chem.* **2008**, *47*, 11. (b) Dincă, M.; Han, W. S.; Liu, Y.; Dailly, A.; Brown, C. M.; Long, J. R. *Angew. Chem., Int. Ed.* **2007**, *46*, 1419.

(14) Chui, S. S. Y.; Lo, S. M. F.; Charmant, J. P. H.; Orpen, A. G.; Williams, I. D. *Science* **1999**, *283*, 1148.

(15) (a) Férey, G. *Chem. Mater.* **2001**, *13*, 3084. (b) Bajpe, S. R.; Kirschhock, C. E. A.; Aerts, A.; Breynaert, E.; Absillis, G.; Parac-Vogt, T. N.; Giebeler, L.; Martens, J. A. *Chem.—Eur. J.* **2010**, *16*, 3926. (c) Kuang, X. F.; Wu, X. Y.; Yu, R. M.; Donahue, J. P.; Huang, J. S.; Lu, C. Z. *Nat. Chem.* **2010**, *2*, 461.

(16) Rouquerol, F.; Roquerol, J.; Sing, K. *Adsorption by Powders and Porous Solids: Principles, Methodology and Applications*; Academic Press: London, 1999.

(17) Gregg, S. J.; Sing, K. S. W. *Adsorption, Surface Area and Porosity*; Academic Press: London, 1982.

(18) *Handbook of Chemical Warfare and Bioterrorism*; Hoenig, S. L., Ed.; Greenwood Press: Westport, CT, 2002.

(19) Ni, Z.; Jerrell, J. P.; Cadwallader, K. R.; Masel, R. I. *Anal. Chem.* **2007**, *79*, 1290.

(20) (a) Rowsell, J. L. C.; Millward, A. R.; Park, K. S.; Yaghi, O. M. *J. Am. Chem. Soc.* **2004**, *126*, 5666. (b) Rowsell, J. L. C.; Yaghi, O. M. *J. Am. Chem. Soc.* **2006**, *128*, 1304.

(21) (a) Sigel, H. *ACS Symp. Ser.* **1989**, *402*, 159. (b) Frey, C. M.; Stuehr, J. In *Metal Ions in Biological Systems*; Sigel, H., Ed.; Marcel Dekker: New York, 1974.

(22) (a) Moss, J. A.; Szczepankiewicz, S. H.; Park, E.; Hoffmann, M. R. *J. Phys. Chem. B* **2005**, *109*, 19779. (b) Rusu, C. N.; Yates, J. T., Jr. *J. Phys. Chem. B* **2000**, *104*, 12292.

(23) (a) Kimura, M.; Nakato, T.; Okuhara, T. *Appl. Catal., A* **1997**, *165*, 227. (b) Inumaru, K.; Ishihara, T.; Kamiya, Y.; Okuhara, T.; Yamanaka, S. *Angew. Chem., Int. Ed.* **2007**, *46*, 7625.

(24) (a) Yang, S. W.; Doetschman, D. C.; Schulte, J. T.; Sambur, J. B.; Kanyi, C. W.; Fox, J. D.; Kowenje, C. O.; Jones, B. R.; Sherma, N. D. *Microporous Mesoporous Mater.* **2006**, *92*, 56. (b) Bromberg, L.; Schreuder-Gibson, H.; Creasy, W. R.; McGarvey, D. J.; Fry, R. A.; Hatton, T. A. *Ind. Eng. Chem. Res.* **2009**, *48*, 1650.